

S. PIETRZYK*, P. PALIMAŁKA*, W. GEBAROWSKI*

THE EFFECT OF LIQUID ALUMINIUM ON THE CORROSION OF CARBONACEOUS MATERIALS

WPLYW CIEKŁEGO ALUMINIUM NA KOROZJĘ MATERIAŁÓW WĘGLOWYCH

During different aluminum smelting processes occur direct contact of liquid metal and carbon materials, which are the main constituent for the lining of the cells, furnaces, crucibles and ladles, etc. As a result, processes of aluminium carbide formation at the interfacial area and its subsequent dissolution occurs. Those are recognized as one of the most important mechanisms causing surface wear and decrease lifetime of the equipment, especially in aluminium electrolysis. Present work is aimed at deeper study of the initial steps of Al₄C₃ formation at the aluminium/ carbon interface. Three types of carbonaceous materials: amorphous, semigraphitic and graphitized, in the presence and absence of cryolite melts, were examined. As it is very difficult to study layer of Al₄C₃ in situ, two indirect experimental techniques were used to investigate aluminium carbide formation: measurements of the potential and the electrical resistance. It was concluded that the process of early formation of aluminium carbide depends on many processes associated with the presence of electrolyte (intercalation, penetration and dissolution) as well as the structure of carbon materials – especially the presence of the disordered phase.

Keywords: aluminium carbide, aluminium electrolysis

Podczas wielu procesów wytapiania aluminium występują bezpośrednie kontakty ciekłego metalu i materiałów węglowych stanowiących wyłożenia wanieli, pieców, tygli i kadzi itp. W rezultacie zachodzą procesy tworzenia węgla glinu na powierzchni międzyfazowej a następnie jego roztwarzania, które są uznawane za jeden z najważniejszych mechanizmów powodujących zużycie powierzchni i obniżenia żywotności urządzeń, zwłaszcza w procesie elektrolizy aluminium. Niniejsza praca miała na celu bliższe poznanie początkowych etapów tworzenia Al₄C₃ na powierzchni granicznej aluminium/węgiel. Zbadano trzy rodzaje materiałów węglowych: amorficzne, semigrafitowe i grafitowe, w obecności oraz przy braku stopionego kriolitu. Ponieważ jest bardzo trudno zbadać warstwę Al₄C₃ bezpośrednio (in situ), zastosowano dwie pośrednie techniki eksperymentalne: pomiar potencjału i rezystancji elektrycznej. Stwierdzono, iż proces powstawania węgla glinu będzie zależeć od wielu zjawisk związanych z obecnością elektrolitu (interkalacja, penetracja i rozpuszczanie), jak również od struktury materiału węglowego a zwłaszcza od obecności fazy nieuporządkowanej.

1. Introduction

Life of an aluminium reduction cell should be as long as possible, as costs are related to relining and loss of metal production. All aluminium smelters are continually trying to increase their production either by increasing the amperage on existing cell designs or designing high amperage cells. This usually means modifications of the materials used in the cell, which in turn can influence the cell life. Selective criteria for cathode base materials are presented in Table 1.

Calcined anthracite has been the primary material used in hall cell linings for many decades. Currently, the advanced technologies, that are under development for high-capacity aluminium electrolysis cells, require the use of refractories for bottom blocks high in carbon materials, pretreated at high temperatures. Current trend is to operate cells with graphitic and graphitized carbon cathode linings [1,2].

TABLE 1
 Selective criteria for cathode base materials [1]

Consideration	Property	Desired trends
Physical properties	Electrical Conductivity	high
	Differential Expansivity	low
	Tensile Strength	high
	Abrasive Resistance	high
	Thermal conductivity	low
Corrosion Resistance	Reactivity with Cryolite	low
	Reactivity with Al and Na	low
	Solubility in Cryolite and Al	low
	Impervious/ porosity	low
	Wettability by bath or metal	low
Economic aspects	Cost	low
	Fabrication	ease
	Jointing	ease

The five main categories of cathode blocks for aluminium reduction cells are [1]:

* AGH UNIVERSITY OF SCIENCE AND TECHNOLOGY, FACULTY OF NON-FERROUS METALS, AL. A. MICKIEWICZA 30, 30-059 KRAKÓW, POLAND

- GCA – gas or kiln calcined anthracite, with 30-50% graphite filler, blocks baked to 1000-1200°C, porosity 16-19%,
 - ECA – electrocalcined anthracite, partly graphitized, with 30% graphite filler, blocks baked to 1000-1200°C, porosity 16-20%,
 - SG – semigraphitic, all aggregates graphitized, baked to 1000-1200°C, porosity 19-23%,
 - SGZ – semigraphitized, graphitizable filler, whole blocks calcined above 2300°C. Porosity 23-26%,
 - GZ – graphitized, baked at 2800°C,
- and they are written in order of an increased graphite character.

Increased and uneven wear of the cathode blocks has accompanied with the increase in current that has taken place in the past decades. Even for the most modern highly efficient technologies, the change in economics of the industry has been generally towards favoring increased productivity at the expense of reduced cathode life. The highest erosion area systematically occurred under anodes at the outer rim, for side break as well as point feeding pots. This phenomenon is called the “W” or “WW” wear profile, and may be due to the convection pattern set up by the movement of the metal pad [3] (Fig. 1). There also seems to be a correlation between the cathodic current density and the wear of the cathode carbon. Thus, during cell life, cathode thickness may be reduced drastically.

The main reason for cell shut-down is cathode wear. The cells are normally operated for about 5-6 years before they are worn out. Considerable costs are connected to the changing of worn cells. These include the cost of disassembly and environmentally sound treatment of spent pot lining, cost of materials and construction of new pot lining as well as lost of productivity.

Aluminium carbide formation and dissolution processes in industrial cells are poorly understood, and several mechanisms have been proposed [4-11]. Generally cathode wear is considered to be a combination of chemical, electrochemical and physical wear mechanisms, all working simultaneously in the cell. It is assumed, that the formation and dissolution of Al_4C_3 are one of the crucial steps of the wear mechanism of carbon cathode blocks in industrial electrolysis cells.

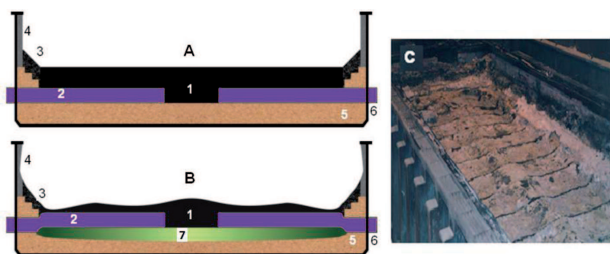


Fig. 1. Cathode autopsy: a) cathode before start-up, b) and c) spent cathode with characteristic WW wear pattern; 1-carbon cathode, 2-steel collector bar, 3- ramming paste, 4-side lining, 5- refractories and insulation, 6- steel shell, 7-“Lens” (bath penetrates the carbon and reacts with the refractories)

Although many laboratory attempts have been made to obtain insight into the problem, the true wear mechanism is still need to be prove. The propose of the present work is

to understand the wear mechanism and to try to develop a realistic evaluation for the cathodic materials.

2. Experimental and results

2.1. Materials

Three sort of cathodic carbon materials: amorphous (ECA), semigraphitic (SG) and graphitized (GZ) (Table 2) were used for measurements. The cathode samples applied in the cell, were machined directly from the commercial grade of carbon blocks (Fig. 2).

TABLE 2
Properties of tested carbon materials (industrial production and testing of properties)

Property	Carbonaceous material		
	ECA	SG	GZ
Density, g/cm ³	1.97	2.16	2.21
Apparent density, g/cm ³	1.61	1.65	1.7
Open porosity, %	13	19	16
Compressive strength, MPa	32	26	35
Flexural strength, MPa	9	8	13
Specific electrical resistivity, $\Omega \cdot \mu\text{m}$	29	16	11
Coefficient of thermal expansion, $\mu\text{m}/(\text{K}\cdot\text{m})$	2.5	2.4	4.2
Thermal conductivity at 30 ⁰ C, W/(K·m)	15	43	125
Ash content, wt.%	3	0.7	0.3

2.2. Techniques

Because of study of aluminium carbide formation in situ is very difficult, two indirect methods were used: measurements of the potential and the electrical resistance. Two test cells were designed. The experimental crucible was installed in a gas-tight kanthal furnace purged with an argon flow.

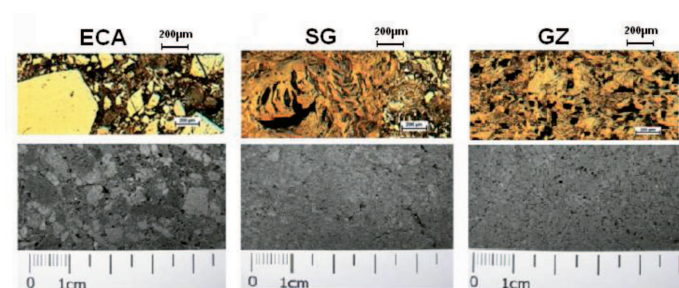


Fig. 2. Surface of the cathodic lining samples

2.3. Potential measurements

The first of the techniques is based on measuring the potential difference (using Keithley 2700 Multimeter/Data Acquisition) between a metallic probe immersed in the metal phase and the carbon bottom of an aluminium electrolysis cell (in the absence of current) [12]. The potential difference was interpreted as the presence of layer of Al_4C_3 , which covered

the contact area between aluminium and carbon. The experimental cell, which is shown in Fig. 3, was designed to see if an “insulating” carbide layer could be formed between the cathodic carbon and a tungsten (W) wire immersed into the liquid metal. The wires were isolated from the bath by sintered alumina tube. The composition of the electrolyte used in the study was as follows: 10 wt. % AlF_3 (CR^{*})=2.26), 5 wt. % CaF_2 , 8 wt. % Al_2O_3 (sat) and 77 wt. % Na_3AlF_6 melted in temperature 965°C (*)CR- cryolite ratio = moles of NaF/moles of AlF_3 , in stoichiometric cryolite (Na_3AlF_6) CR=(3 moles of NaF/1 mole of AlF_3) =3).

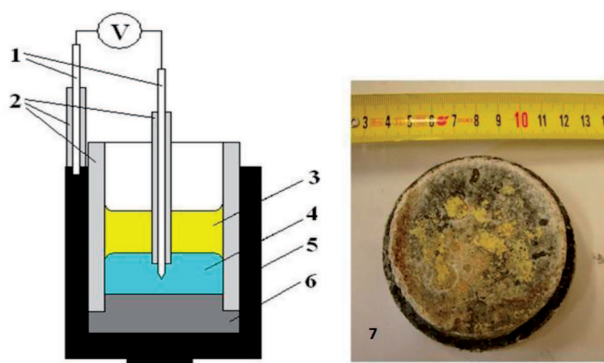


Fig. 3. Experimental cell: 1- W wire, 2- sintered alumina tubes, 3- electrolyte, 4- aluminium, 5- carbon crucible, 6- sample of carbon lining, 7- appearance of the sample after test

After the stable potential difference (~120 mV) was reached, pointed Mo wire was pressed against the bottom of the crucible (Fig. 4 situation B). The potential difference then showed a sudden drop of about 80 mV (in anodic direction). It was interpreted as a result of penetration and partly “short circuiting” of an “insulating” layer at the Al/ Al_4C_3 carbon interface. When the pointed Mo wire was removed from the surface of cathode lining (Fig. 4 situation A) a sudden change of potential was observed (about 40 mV). The shift of the potential back to its stable value suggests that the “self repairing” process of Al_4C_3 layer was very slow.

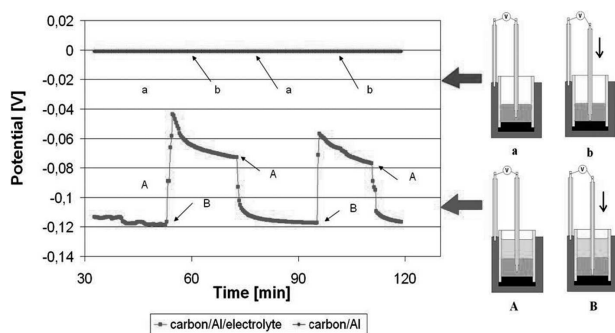


Fig. 4. Principles of experimental technique and example of results of potential measurements (ECA sample)

2.4. Resistance measurements

The second technique involved measurements of the electrical resistance changes (based on Ohm’s Law) between two Mo probes using dc current provided by Sorensen DCS60-50E power supply. The experimental cell, presented in Fig. 5 was used to measure changes of resistance (Fig. 6 and 7) caused

by the formation of Al_4C_3 layer in four systems: a). carbon/Al/electrolyte; b). carbon/Al; c). carbon/electrolyte; and d). “short circuit” of Mo electrode on cathodic carbon. All systems were investigated at the same time, with the same conditions.

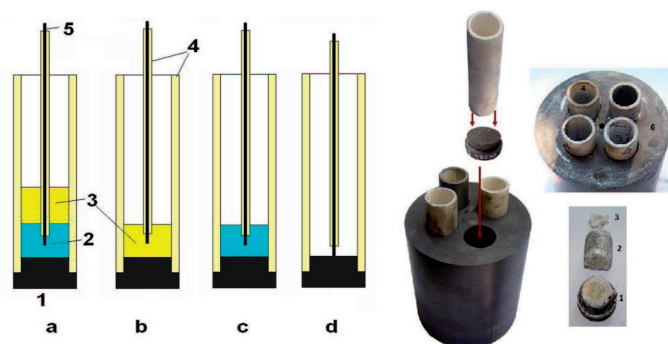


Fig. 5. Details of experimental cell for resistance measurements: 1- carbon lining sample, 2- aluminium, 3- electrolyte, 4- sintered alumina tube, 5- Mo wire, 6- graphite crucible, used in four systems: a)- carbon/Al/electrolyte; b)- carbon/electrolyte; c)- carbon/Al; and d)- “short circuit” of Mo electrode on cathodic carbon

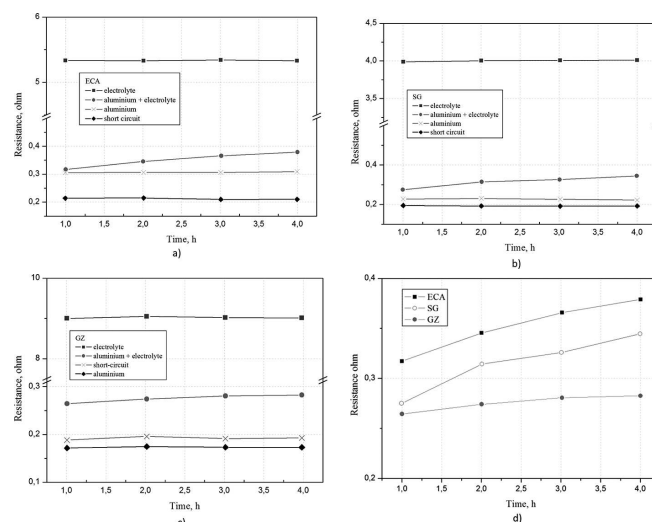


Fig. 6. Changes of electric resistance for: a) ECA; b) SG; c) GZ in four systems, and d) resistance comparison of tested samples in system with aluminium and electrolyte

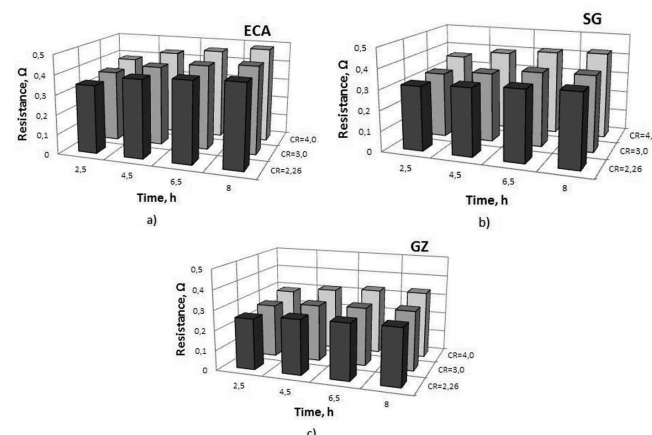
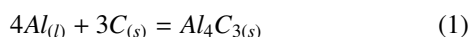


Fig. 7. Influence of the melt composition on the resistance changes in C/Al/electrolyte system for: a) ECA, b) SG and c) GZ

To determine the effect of electrolyte composition on the formation of carbide layers, measurements were carried out in the same measuring vessel as described previously (system a). The melts had a CR = 2.2; 3.0 and 4.0. Results are presented in Fig. 7.

3. Discussion

Thermodynamics indicate that aluminium and carbon should react to form aluminium carbide:



The standard Gibbs formation energy of Al_4C_3 is -138.76 kJ at 965°C ($E^0 = -119.93$ mV). The reaction is thermodynamically favored at all temperatures of interest in aluminium electrolytic production. However, in spite of this large negative formation energy, aluminium and carbon appear to be mutually "nonreactive" at normal electrolysis temperatures. In experiments with liquid Al in contact with carbon the amount of carbide suggested by the thermodynamics was not readily found. There was no potential drop observed between Mo electrodes during pressing/ raising of Mo wire against/from the surface of cathode lining (Fig. 4. situation a and b). The distinctive, brightly yellow layer of Al_4C_3 on surface of cathode samples was not observed after experiment. The protective oxide layer on the aluminium evidently prevents the metal from directly contacting the carbon, thereby making the reaction dependent on diffusion across a carbon/ Al_2O_3 /Al interface. On the other hand, in the presence of molten cryolite, aluminium easily reacts with carbon, forming Al_4C_3 (measured potential values were close to E^0 for the equation (1)). Similar behavior, as in the ECA sample presented in Fig. 4, were obtained for other studied cathode materials. The catalytic role of cryolite can be ascribed to a fluxing action, causing dissolution of the protective aluminium oxide layer and allowing the metal to "wet" the carbon. The measured resistance is the sum of resistances in series: molten aluminium, the electrolyte layer between the carbon and aluminium, layer of solid Al_4C_3 on the surface of the carbon sample. The results show that the resistance values do not change during the experiment in the systems: with aluminium, with electrolyte and short-circuited (system b, c and d). Resistance increase in system (a) is clearly due to formation of the Al_4C_3 layer only in the presence of an electrolyte. The increase of resistance may be also due to formation of Al_4C_3 layer on the surface of carbon and its dissolution into the electrolyte. Aluminium carbide will act as a very thin, low conducting electric barrier at the interface, thus enabling a potential drop across it.

Figure 8 shows a comparison of measured resistivity components in the system (C / Al / bath).

As can be seen, the greatest impact on the resistance should have Al_4C_3 created on the surface of carbon. The second component, which may have an impact on the value of the measured resistance, is the electrolyte. Figure 9 presents the results of calculations on the percentage increase in resistance (ΔR) of the electrolyte saturated with Al_4C_3 in relation to the bath without carbide (based on the known empirical equations [14]) and increase of the resistance measured in the systems (C / Al / electrolyte) for the tested samples.

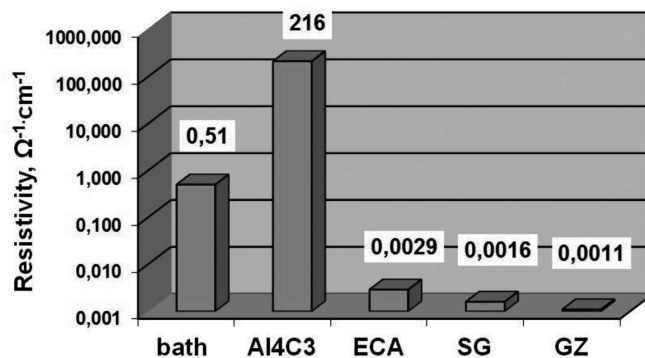


Fig. 8. Comparison of resistivity of the materials occurring in the measurement systems (resistivity Al_4C_3 from [13])

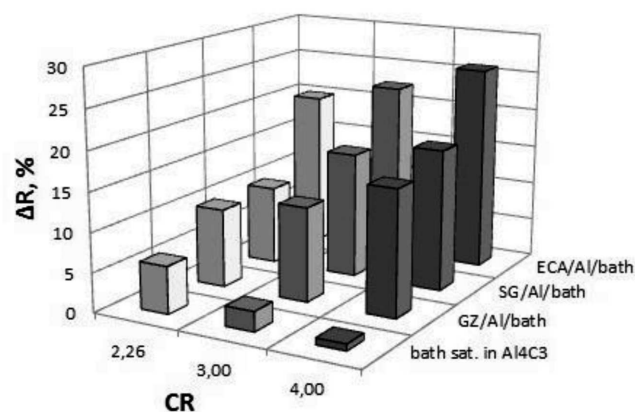
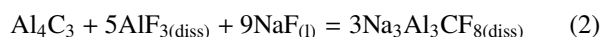


Fig. 9. Impact of CR on the increase of the resistance (ΔR) of the electrolyte saturated in Al_4C_3 [14] and the resistance in the whole system carbon / Al / bath

As can be seen from the results shown in the Fig. 9, the composition of the electrolyte also has an impact on resistance of the investigated system. The increase of CR causes an increase in measured resistance for all tested carbon materials. As shown in Fig. 9, bath saturated in Al_4C_3 can also cause deterioration of the electrolyte conductivity and an increased resistance of the bath layer, but its impact will be opposite to the entire system (i.e. decrease of ΔR with increase of CR). It is known that with increasing CR decreases the solubility of Al_4C_3 in the electrolyte according to the reaction (2):



Solubility of Al_4C_3 at 965°C is 0.64 wt.%, 0.31 wt.%, and 0.13 wt. % for CR = 2.26; 3.0 and 4.0 respectively [14]. At the same time in the system there are growth of the Al_4C_3 layer and its dissolution into the electrolyte. Both of these phenomena affect the thickness of the carbide layer and its resistance, as well as resistance of the electrolyte. Increased solubility of carbide will cause the formation of thinner films and lower resistance for current passing. The increase in thickness of aluminium carbide layer during the experiment can take place only if the saturation of aluminium carbide in electrolyte is reached, or the rate of dissolution of Al_4C_3 is lower than rate of its formation.

If the formed aluminium carbide is transported away from the cathode surface it allows new surfaces to react. This can be done in three ways:

- I. Dissolution of the film presented between the cathode and the aluminium pool into the bath. Aluminium carbide has significantly higher solubility in the bath (approximately 100 ppm at reduction cell temperature [15,16]) than in metal, and hence the rate of carbide removal will be enhanced in region where the carbon surface is more likely to be accessed by bath. Both industrial observations (the cathode block is always fully penetrated with bath) and laboratory observations indicate that such a bath film is indeed present. The carbide saturated bath film will need to be replaced with “fresh” electrolyte, which can dissolve more carbide. Marangoni flow is a phenomena that explains exchange of electrolyte from bulk bath with a thin film under the metal pad. The Marangoni effect (also called the Gibbs-Marangoni effect) is the mass transfer along the interface between two fluids due to surface tension gradient. Since a liquid Al with a high surface tension (819 mN/m at 965⁰ C [17]), pulls stronger on the surrounding liquid bath than one with a low surface tension (102 mN/m at 965°C [17]) the presence of a gradient in surface tension will naturally cause the bath to flow away from regions of low surface tension. This introduces “fresh” bath, thus increasing the dissolution of the carbide layer.
- II. Dissolution into the metal. Measurements of the carbon content in the metal in industrial cells have shown that the metal is always far from saturation [15,16]. Due to the presence of an electrolyte layer on the surface of carbon the first process before carbide dissolution in the electrolyte must be its transport to the surface of the aluminium. Hence the step, which determine the rate, must be either dissolution of carbide in the layer of electrolyte or dissolution of carbide in the metal.
- III. Hypothetical process – spalling and buckling of carbide layer. It was first proposed by Siew et al. [18], that the carbide layer formed on the cathode is comparable to an oxide layer formed on metal surface. Such phenomena can be described by Pilling-Bedworth ratio (R_{P-B}), and can be defined as the volume of carbide formed divided by the volume of aluminium required to produce that volume of carbide:

$$R_{P-B} = \frac{V_{Carbide}}{V_{cm}} = \frac{M_{Carbide} \cdot d_{cm}}{n \cdot M_{cm} \cdot d_{Carbide}} \quad (3)$$

where : M – the atomic or molecular mass, n – number of atoms of metal per one molecule of the carbide, d – density, V – the molar volume, cm – tested carbon materials.

The Pilling-Bedworth ratio for forming aluminium carbide on the carbon surface was calculated to be over 2, which suggest that the formed carbide layer is a non protective layer. It can be noted that based on different densities of studied materials, R_{P-B} of carbide is slightly different ($R_{P-B} = 2.48$; 2.72 and 2.79 for ECA, SG and GZ, respectively). The compressive stress in the carbide layer will force the carbide layer to spall off if it is brittle or buckle off if is elastic (Fig. 10).

However, this hypothesis requires further experimental studies to confirm the theoretical calculations. Measured resistance decreases in sequence amorphous, semi-graphitic and graphitized materials. Resistance of graphitized material (GZ)



Fig. 10. Spalling carbide layer as a result of compression ($R_{P-B} > 2$)

is the lowest. For CR = 2.26 and for GZ material occurs the lowest increase in measured resistance. This may indicate that the formed carbide layer is the thinnest. This may be a result of two reasons. First, due to the fact that this electrolyte (CR=2.26) has the largest Al_4C_3 solubility among tested bath. The other reason, may result from the structure of the carbon material, in this case – the contents of disordered carbon phase. The second reason decides on the value of the measured resistance and its growth. Previously it was believed that carbide formation is independent of the cathode carbon grade/type [7]. However, present laboratory work has shown that the electrochemical formation of carbide layer is more favoured for disordered carbons (i.e. antracitic versus graphite). The same conclusions were formulated by Rafiei et al. [19]. They concluded that electrochemical formation of aluminium carbide is thermodynamically more favoured for disordered carbons, which have a thermodynamic activity greater than unity and, therefore reaction of that material would be favoured over graphite, when both are present at given location. According to Reny and Wilkening [20], more disordered and less graphitic structures (e.q. calcined antracite) are more resistant to electrochemical wear, as the adhesion of aluminium carbide may be stronger compared to more ordered structures. Changes of electrical resistivity of graphitized cathode block during and after electrolysis was measured by Sato et al. [21]. When the sample was applied as the cathode, the electrical resistivity of the sample showed sudden decrease immediately after electrolysis started. Upon interruption of electrolysis, the resistivity showed sudden increase and was back to the level before electrolysis. The authors explained such behavior as follows: during electrolysis the intercalation of sodium into cathode sample leads to decrease of electrical resistivity. After the interruption of the electrolysis, decomposition of intercalated compounds occurred. However, those results are difficult to compare with these presented in this work, which were obtained under conditions of no current flow. To sum up it can be concluded that the process of early formation of aluminium carbide will depend on many processes associated with the electrolyte (intercalation, penetration and dissolution) as well as the structure of cathode lining and especially the presence of the disordered phase. A deeper understanding of aluminium carbide formation mechanism requires further studies.

Acknowledgements

Financial support by a grant PL 0269 from Iceland, Liechtenstein and Norway through the EEA Financial Mechanism and the Norwegian Financial Mechanism as well as Polish Ministry of Science and Higher Education is gratefully acknowledged.

REFERENCES

- [1] M. Sørli, H.A. Øye, Cathodes in Aluminium Electrolysis, Aluminium-Verlag, Düsseldorf, (1994).
- [2] M. Sørli, H.A. Øye, J. Appl. Electrochem. **19**, 580 (1989).
- [3] D. Lombard, T. Béhérégaray, B. Fève, J.M. Jolas, Light Metals. 653 (1998).
- [4] J. Xue, H.A. Øye, Light Metals. 211 (1994).
- [5] X. Liao, H.A. Øye, Light Metals. 667 (1998).
- [6] X. Liao, H.A. Øye, Light Metals. 621 (1999).
- [7] K. Vasshaug, The Influence of the formation and dissolution of aluminium carbide on the cathode wear in aluminium electrolysis cell, PhD. Thesis, Norwegian University of Science and Technology, Trondheim, Norway, (2008).
- [8] S. Pietrzyk, P. Palimaka, Materials Science Forum. 2438 (2010).
- [9] B. Novak, K. Tschöpe, A.P. Ratvik, T. Grande, Light Metals. 1343 (2012).
- [10] B. Novak, K. Tschöpe, A.P. Ratvik, T. Grande, Light Metals. 1245 (2013).
- [11] B. Novak, On the chemical and electrochemical formation of aluminium carbide in aluminium electrolysis. PhD thesis, Norwegian University of Science and Technology, Trondheim, Norway, (2013).
- [12] S. Rolseth, E. Skybakmoen, H. Gudbrandsen, J. Thonstad, Light Metals. 423 (2009).
- [13] W.R. King, R.C. Dorward, J. Electrochem. Soc. 132, 388 (1985).
- [14] R. Odegard, On the solubility and electrochemical behaviour of aluminium and aluminium carbide in cryolitic melts. Dr. Techn. thesis, Norwegian Institute of Technology, University of Trondheim, Norway, (1986).
- [15] R.C. Dorward, Metall. Trans. **21A**, 255 (1990).
- [16] J. Rodseth, B. Rasch, O. Lund, J. Thonstad, Light Metals. 883 (2002).
- [17] J. Thonstad, P. Fellner, G.M. Haarberg, J. Hives, H. Kvande, A. Sterten, Aluminium electrolysis, Aluminium-Verlag, Düsseldorf, (2001).
- [18] E.F. Siew, T. Ireland-Hay, G.T. Stephens, J.J.J. Chen, M.P. Taylor, Light Metals. 763 (2005).
- [19] P. Rafiei, F. Hiltmann, M. Hyland, B. James, B. Welch, Light Metals. 747 (2001).
- [20] P. Reny, S. Wilkenning, Light Metals. 399 (2000).
- [21] Y. Sato, H. Imagawa, N. Akuzawa, Light Metals. 979 (2008).